

Activating a Silver Lipoate Nanocluster with a Penicillin Backbone Induces a Synergistic Effect against *S. aureus* Biofilm

Humberto H. Lara,^{*,†,‡} David M. Black,^{‡,⊥} Christine Moon,[§] Elizabeth Orr,[§] Priscilla Lopez,[‡] Marcos M. Alvarez,^{*,§} Glen Baghdasarian,[§] Jose Lopez-Ribot,[‡] and Robert L. Whetten^{*,||}

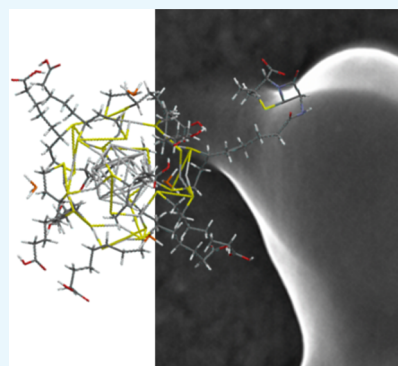
[†]Department of Biology and South Texas Center for Emerging Infectious Diseases and [‡]Department of Physics & Astronomy, University of Texas, San Antonio, Texas 78249, United States

[§]Department of Chemistry, Los Angeles City College, 855 N Vermont Ave, Los Angeles, California 90029, United States

^{||}Center for Materials Interfaces in Research & Applications (MIRA), Applied Physics and Material Science, Northern Arizona University, Flagstaff, Arizona 86011, United States

S Supporting Information

ABSTRACT: Many antibiotic resistances to penicillin have been reported, making them obsolete against multiresistant bacteria. Because penicillins act by inhibiting cell wall production while silver particles disrupt the cell wall directly, a synergistic effect is anticipated when both modes of action are incorporated into a *chimera* cluster. To test this hypothesis, the lipoate ligands (LA) of a silver cluster (Ag_{29}) of known composition ($\text{Ag}_{29}\text{LA}_{12}$)^[3-] were covalently conjugated to 6-aminopenicillanic acid, a molecule with a β -lactam backbone. Indeed, the partially conjugated cluster inhibited an *Staphylococcus aureus* biofilm, in a dose–response manner, with a half-maximal inhibitory concentration IC_{50} of 2.3 μM , an improvement over 60 times relative to the unconjugated cluster ($\text{IC}_{50} = 140 \mu\text{M}$). An enhancement of several orders of magnitude over 6-APA alone (unconjugated) was calculated ($\text{IC}_{50} = 10\,000 \mu\text{M}$). Cell wall damage is documented via scanning electron microscopy. A synergistic effect of the conjugate was calculated by the combination index method described by Chou–Talalay. This hybrid nanoantibiotic opens a new front against multidrug-resistant pathogens.



INTRODUCTION

Bacterial infections are the most important cause of morbidity and mortality worldwide, and in most cases the principal isolate is *Staphylococcus*.¹ The main characteristic of *Staphylococcus aureus* is its capability to easily gain resistance against almost all antimicrobials.² 6-APA is the nucleus and the precursor for creation of semisynthetic penicillins.³ Penicillin acts against susceptible *S. aureus* by targeting the transpeptidase that catalyzes the last stage in the bacterial cell wall biosynthesis (peptidoglycan). The bacterial cell wall is the rigid structure that maintains the characteristic form of the bacteria and shelters against osmotic cell lysis.⁴ Silver nanoparticles (AgNPs) are the most studied antimicrobials in nanotechnology demonstrating potent broad-spectrum activity.^{5,6} The AgNP targets permeability of the bacterial cell membrane, then after penetrating the cell, alters sulfur-containing amino acids and phosphorus (DNA), hindering replication. Previous research based on advanced electron microscopy showed that the positively charged AgNPs induce wall thinning, pore formation, leakage of cell content, and finally cause cell lysis.^{7–9} Once inside the cell, the silver nanoparticles fall apart and generate highly reactive silver species responsible for antimicrobial activity.^{5,10–13}

A silver cluster comprising 29 Ag atoms and 12 lipoate ligands (hydrodynamic diameter of 3 nm) was recently

reported to be active against methicillin-resistant *S. aureus* bacteria (MRSA) and preformed *Candida albicans* biofilms.¹⁴ However, the modest inhibitory concentrations reported in that study (140 μM level) limit the use of the clusters to biomedical applications. Although small, the cluster has a 13-atom metallic icosahedral core responsible for the antimicrobial activity. Further size reduction results in inert nonmetallic oligomeric structures that exhibit reduced activity.¹⁵ Conversely, larger silver particles ($D > 10 \text{ nm}$) have a larger metallic core and are known to inhibit at lower concentrations (IC_{50} 0.4–3.2 $\mu\text{g/mL}$).^{16,17} However, small silver particles ($D < 6 \text{ nm}$) afford advantages of enhanced stability and renal clearance with rapid and efficient urinary excretion.^{18–21}

A promising approach to enhance the antimicrobial activity of the cluster is to conjugate its ligands to a penicillin nucleus.³ As a proof of concept, 12 pendant carboxylates of lipoic acid ligands in $\text{Ag}_{12}(\text{LA})_{12}$ ^[3-] may be covalently coupled (conjugated) to a penicillin nucleus known as 6-aminopenicillanic acid (6-APA). An intermediate of penicillin biological degradation,^{22,23} 6-APA itself is ineffective but retains the essential β -lactam backbone structure. The

Received: September 6, 2019

Accepted: November 27, 2019

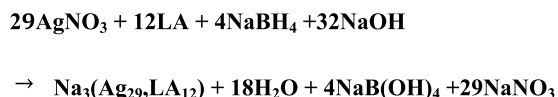
Published: December 13, 2019

conjugated cluster is, thus, expected to combine both the mode of action of penicillins (inhibition of biosynthesis of cell wall muropeptide)²⁴ and the mode of action of silver nanoparticles (cell wall disruption and lysis) while retaining the advantage of rapid kidney elimination exhibited *in vivo* by small clusters.²¹

RESULTS AND DISCUSSION

Chemistry. Claims of covalently conjugating penicillin to nanoparticles abound in the literature.^{25–29} However, in most cases, proof of conjugation is provided only indirectly through bioassays because large nanoparticles are not amenable to analysis by mass spectrometry, the most useful analytical technique for quantifying conjugation. For that reason, the few reports that provide direct evidence of linkage through an amide bond are for small clusters.^{30,31} One of the earliest reports demonstrated that a known gold cluster molecule (“Undecagold” Au₁₁(PPh₃)₇I₃) could be obtained in a water-soluble form and modified by conjugation of the Ph*⁺-groups to biomolecular groups.³² It formed abundantly because it has eight (8) extra or “free” electrons that occupy a closed-shell s²p⁶ configuration of globular “superatomic” orbitals.³³ The 29-Ag cluster employed here as a starting reagent similarly exhibits an 8-electron closed-shell electronic structure responsible for its remarkable yield and stability that facilitates further processing, such as conjugation. *R*- α lipoic acid (LA or RALA), also known as thiocctic acid, is a natural product (an enzyme cofactor essential to aerobic metabolism); as a dithiolate, it has a high affinity to noble metals (Au, Ag, ...). The Ag lipoate (29, 12) cluster is abundantly produced via a borohydride reduction, as summarized in Scheme 1:^{14,34–36}

Scheme 1. Reduction of Silver Salt by Sodium Borohydride in the Presence of Lipoate (LA) Ligand under Alkaline Conditions^a



^aLA and reducing agent are added in 2.5:1 molar excess relative to silver.

The chemistry for conjugating a carboxylate group to an amine group has been amply described in the literature.^{31,37,38} The major role that lipoic acid plays in biological reactions has motivated extensive research in conjugating it to molecules of therapeutic interest.^{39–43} The reaction employed in this study is summarized in Scheme S1 of the Supporting Information. Evidence of conjugation of 6-APA to the cluster is provided here (Figure 1B) by electrospray ionization mass spectrometry (ESI-MS). The ESI-MS signal from the unconjugated cluster is observed at a mass-to-charge ratio that corresponds with isotopic resolution^{6,14} to its triply charged state [3⁻], as expected from its natural ionized state (Scheme 1).

Like oligonucleotides, metal clusters show a propensity to form adducts; this is evident from Figure 1A that shows the presence of sodium and/or triethylammonium cations substituting the carboxylic hydrogen in the lipoic acid terminus. Nevertheless, the signal from the parent cluster dominates the spectra indicating that any antimicrobial activity is attributable to the Ag₂₉LA₁₂^[3⁻] complex.

It is of interest to note that as expected when the spectrometer is operated in negative mode, the signal

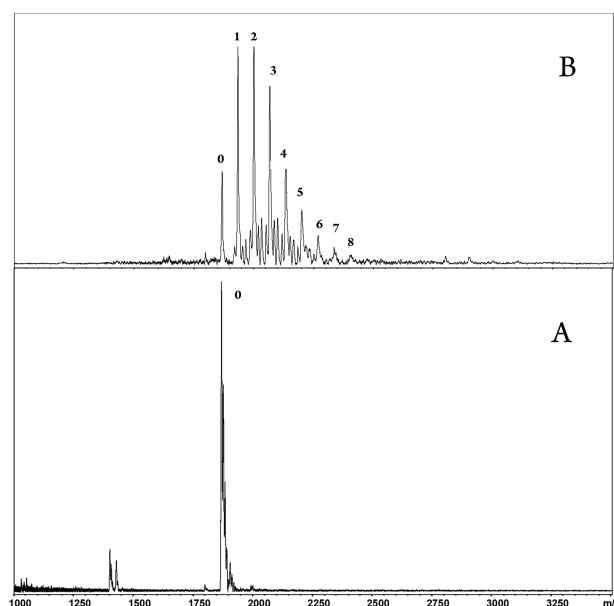


Figure 1. Negative mode ESI-MS of the cluster (Ag₂₉LA₁₂)^[3⁻] [~5.6 kDa] before (A) and after (B) conjugation. (A) ESI-MS for the unconjugated cluster (triply charged) labeled with the number of 6-APA groups ($p = 0, 1, 2, 3, \dots, 7, 8, \dots, 12$ -max). The adducts in the first spectrum (no reaction) are sodium and triethylamine. (B) Evidence for the conjugation of up to eight lipoic acid ligands. The bare triply charged parent mass is observed at 1867.9 amu at 10% abundance. The remaining 90% of clusters are conjugated.

corresponds to some ligands being deprotonated (as lipoates) or, to a lower extent, neutralized by a cation adduct (lipoate salts). Solubility in aqueous solution requires the deprotonated charge state (lipoate). This observation is significant because pH plays a fundamental role in its conjugation chemistry and on its use as an antimicrobial agent.^{38,44} The cluster must remain in aqueous solution at physiological pH and ionic strength.

The cluster Ag₂₉LA₁₂^[3⁻] was conjugated in a two-step process, as detailed in Schemes S1 and S2 of the Supporting Information and summarized in the Experimental Section. Crucially, the efficiency of the coupling reaction was increased remarkably using the free-base form of the coupling agent and by increasing the buffering capacity [2-(*N*-morpholino)ethanesulfonic acid, MES, 500 mM]. Much lower yields were observed when 50 mM MES was used, all other parameters being equal.

Post-reaction, the ESI-MS spectrum (Figure 1B) shows evidence that over 90% of the clusters are coupled to the penicillin precursor, i.e., the signal from the parent unconjugated cluster ($N = 0$) is less than 10% of the total signal (Figure 1B) as judged from integrating the areas under each peak. It is evident that up to 8 ligands per cluster have been conjugated out of a maximum of 12 ligands. The abundance from the conjugated clusters conforms to a slightly long-tailed distribution with a mean of 2.7 and a standard deviation of 1.6.

Partial conjugation at the level demonstrated in Figure 1 may be advantageous relative to full conjugation. The cluster remains water soluble (the conjugated ligands are less polar and nonionizable). In addition, the cluster retains the lipoic acid moiety that is compatible with the phospholipid bilayers of the pathogenic targets, an essential feature that allows the

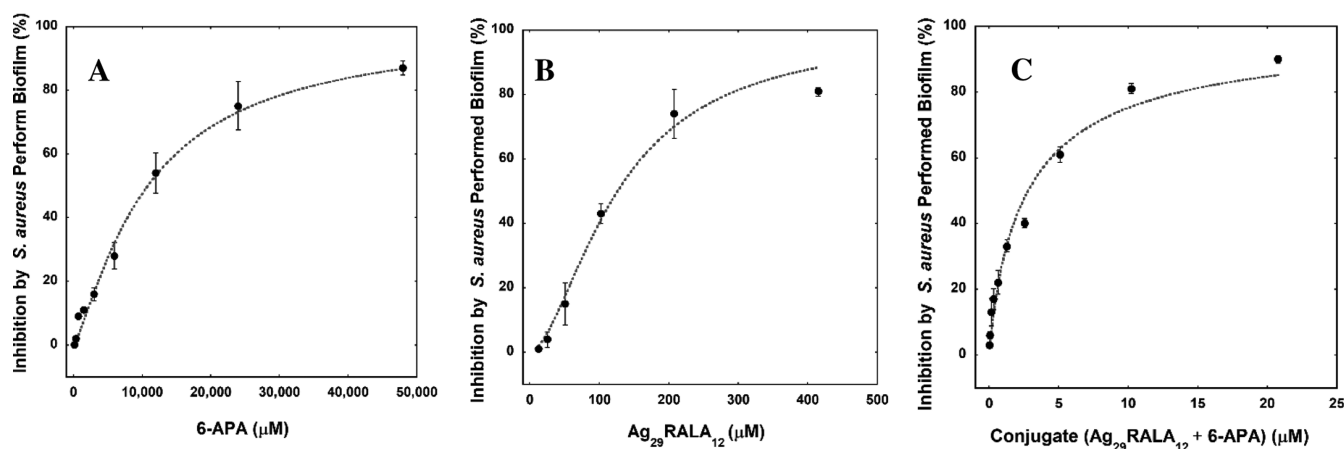


Figure 2. Phenotypic assay for *S. aureus* preformed biofilm inhibition. (A) Inhibition by 6-APA, (B) inhibition by Ag_{29} cluster, and (C) inhibition of the cluster conjugate (Ag_{29} + 6-APA). Error bars represent \pm standard deviation (SD) from the mean of three independent assays in duplicates each.

cluster to approach the cell wall and membrane. Indeed, these solubility effects are noticeable and put to good use in the workup procedure. The first steps of conjugation (Scheme S1) lead to the formation of a stable ester that precipitates from the reaction due to its lower solubility facilitating its isolation and the removal of isoureas side products and other impurities from the activation reaction. In addition, isolating the stable NHS [*N*-hydroxysulfosuccinimide] ester is important because it allows for the amidation reaction to occur at a higher more favorable pH.³⁸

The solubility of the cluster also decreases as each free carboxylate anion is replaced by an amide bond as conjugation proceeds. The conjugated cluster precipitates from solution, and thus allowing the removal of additional impurities. Increasing the pH deprotonates unconjugated ligands and the cluster becomes soluble once again. Although the antibacterial action of the conjugated cluster is expected to increase with an increasing degree of conjugation, the advantages discussed above would be compromised. It is also important to note that higher reaction pH minimizes the degradation of the β -lactam ring that occurs at lower pH.^{45,46}

To optimize reaction conditions with an amine more stable than 6-APA, the conjugation reaction was performed with glycine ethyl ester as a 6-APA surrogate. Surprisingly, the glycine ethyl ester also attaches to up to eight lipoic acid ligands. A much stronger ESI-MS signal (as shown in the Supporting Information) was observed, albeit with monotonous decaying abundances. Conjugation of eight ligands leaves four ligands in the native lipoate form. In addition to imparting solubility and biocompatibility to the clusters, four ligands may play a role as four internal coordinating ligands essential for the stabilization of the tetravalent cluster.^{4,47}

The total structure of the bare aqueous cluster is not known but is inferred from theoretical calculations that take the structure of the nonaqueous homolog as a starting point.⁴⁷ Theoretical calculations¹⁴ reveal the presence of four electron-deficient silver atoms tetrahedrally arranged at the surface of the cluster that are stabilized by weakly coordinated ligands in the nonaqueous analog.⁴⁷

In continuing work, it will be possible to isolate specific species with a fixed number of conjugated ligands using high-performance liquid chromatography, as demonstrated and detailed in the Supporting Information in the conjugation of

glycine ethyl ester to the cluster. This will allow the efficacy and stability to be studied systematically as a function of the extent of conjugation (from one to eight or more ligands). Other antimicrobials or moieties with a free amine group may conjugate to Ag_{29} . For example, ampicillin was successfully conjugated following the protocol (Figure S1 in the Supporting Information).

Biological Evaluation. By a luciferase assay, we obtained the IC_{50} for 6-APA, Ag_{29} cluster, and the conjugate against the *S. aureus* biofilm as follows: 10 000, 140, and 2.3 μM , respectively (Figure 2).

6-APA alone needs a large quantity of the compound to inhibit, as it is only a nucleus used to develop a new generation of penicillins, and the Ag_{29} cluster has effectivity against the biofilm in the order of micrograms. The conjugate (Ag_{29} + 6-APA) requires a small quantity of the cluster to be effective.

The mechanism of antimicrobial action of nanoparticles, in general, has been amply studied and reviewed.⁴⁸ What sets the subject cluster apart is its enhanced efficacy and versatility attributed to the synergetic effect of its individual components in attacking the microbial cell wall (CW) and cell membrane. The bioaffinity of the lipoate ligand allows the cluster to permeate microbial biofilms, CW, and phospholipid membranes. In addition, the β -lactam moiety of penicillanic acid derivatives allows the clusters to weaken the microbial CW. Once the microbial defenses are broken, the cluster disintegrates into silver ions with the concomitant generation of reactive oxygen species² that degrade the cell's DNA and protein, essential to the microbes' existence.

The increased antimicrobial activity of the conjugated cluster can be explained as activation of the cluster or as activation of the β -lactam backbone. An example of the latter is provided by the coupling of 6-APA to borane clusters that results in increased activity against *S. aureus*.⁴⁹ Combination drug therapy is the action of many drugs in combination to achieve synergy; this is frequently used against antibiotic-resistant infections. Synergy is defined as the interaction of two or more antibiotics to achieve a combined antimicrobial effect greater than the summation of their efficacies alone. The theorem of Chou–Talalay⁵⁰ uses algorithms for automated computer simulation to quantitatively measure synergy, as shown in a plot of the degree of inhibition or fractions affected (Fa) versus combination index (CI).⁵¹ The index compares

the inhibition predicted by the mass-action law when the components are combined at various proportions to the actual inhibition observed at the same proportions. An index of one indicates an additive effect. Synergism is indicated when the index is less than one. Antagonism is indicated when the index is greater than one.

To corroborate that the conjugate has a synergistic effect compared with the effect of Ag₂₉ or 6-APA alone, we implemented the Chou–Talalay method⁵⁰ using the CompuSyn 1.0 software. A constant mixing proportion of 2.7 moles of 6-APA to 1 mole of the cluster was estimated from the average degree of conjugation experimentally determined from the mass spectra (2.7 ligands/cluster, Figure 1). Knowledge of the cluster composition (Scheme 1) allows the calculation of the molarity of the cluster used to report antibiotic dose. The Fa–CI plot from the computer simulation is presented in Figure 3

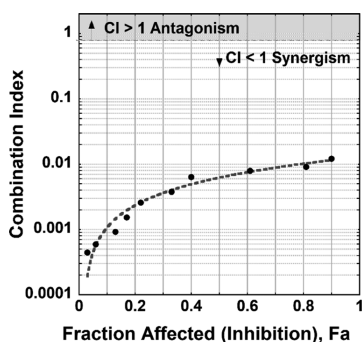


Figure 3. Fa–CI plot. The data are the mean values from three independent experiments. Combined doses of the conjugate (Ag₂₉ cluster and 6-APA antibiotic) ranging from 0.032 to 20.8 μ M, resulted in CI < 1 (synergy) ranging from 0.00044 to 0.012. Combination indexes are plotted on a logarithm scale for easy comparison to the CI = 1 limit between synergistic or antagonistic effects.

and detailed in Table S1 in the Supporting Information. Median dose (IC₅₀) and other parameters reported by curve fitting the phenotypic assay results (by the CompuSyn 1.0 program) are summarized in Table S2. All doses used in this

test for the Ag₂₉–6-APA conjugate demonstrated a synergist effect.

To visualize the ultrastructural effect of the cluster, 6-APA, and the conjugate against the *S. aureus* biofilm, we used scanning electron microscopy (SEM), the nontreated cells were abundant, clustered, round, with a smooth surface and with some extracellular polymeric substances (EPSs) characteristic of the biofilm (Figure 4a). After 24 h treatment with Ag₂₉, some cells become distorted and AgNPs accumulate on the EPS (Figure 4b). Bacterial cells treated with 6-APA have mild distortions on the outer cell surface of the membrane (Figure 4c). After treatment with the conjugate, the cells become distorted, with disruption of the outer cell membrane and leakage of the cell content (red arrows), as shown in Figure 4d.

It should be noted that the microbiological assay reported here was NOT performed against a methicillin-resistant *S. aureus* bacteria (MRSA). However, the assay was performed against a preformed biofilm, which is more antibiotic resistant than in the planktonic form. In future work, we anticipate a similar enhancement in activity when the conjugated cluster is tested against MRSA.

The antimicrobial efficiency of the cluster can be further optimized by controlling the cluster charge, the degree of conjugation, the length and shape of the penicillanic acid derivative, and the cluster concentration. Furthermore, once absorbed into the microbe, the cluster activity can be controlled by judicious exposure to light, heat, and pH. The conjugated cluster may be used in topical applications (i.e., wound infections, surface disinfection, catheter protection).

CONCLUSIONS

Incorporation of a β -lactam moiety (6-APA) to a silver cluster of known composition results in a 60-fold enhancement in its activity against a preformed *S. aureus* biofilm, as demonstrated by in vitro susceptibility methods and electron scanning microscopy. Evidence for conjugating and averaging of 2.7 ligands per cluster and up to eight ligands is supported by electrospray ionization mass spectrometry.

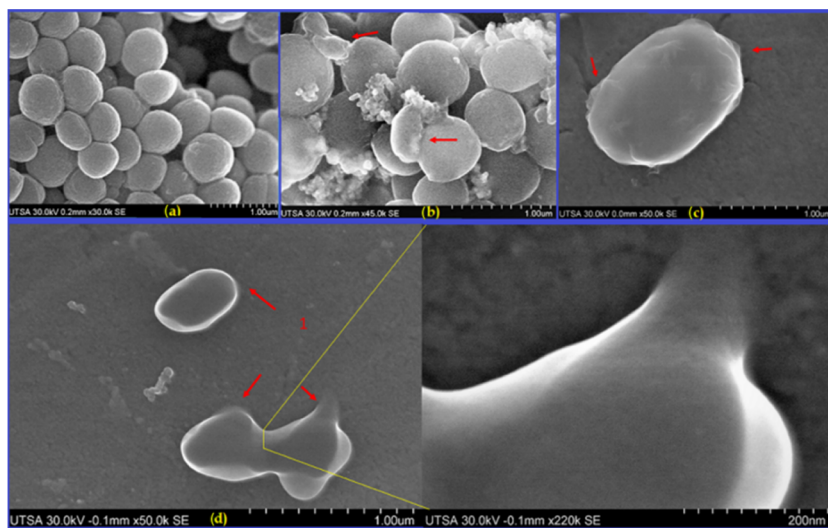


Figure 4. SEM microscopy of the *S. aureus* preformed biofilm. (a) Untreated preformed biofilm, (b) preformed biofilm treated with Ag₂₉ clusters at concentration, (c) biofilm after 6-APA treatment at 12 mM, (d) preformed biofilm of *S. aureus* after 24 h treatment with the conjugate (0.11 mM). Red arrows indicate disruption of the outer cell membrane.

Ongoing work includes conjugation of the ligand in the organic phase, cluster conjugation via ligand substitution reactions, and testing antimicrobial activity against MRSA superbugs and against a wider range of substrates. In addition, the conjugation of the isolated ligand and its subsequent incorporation into the cluster via place exchange reactions is being investigated. The methods described here are significant because they may be extended beyond penicillins to a plethora of existing antiviral agents or other antibacterial agents with different modes of action. The application of other coupling modes (disulfides, organosilanes, phosphate esters, etc.), other metals with antimicrobial activity (Cu), and the alloying of clusters with biocompatible metals (Ti) is also within reach.

■ EXPERIMENTAL SECTION

Cluster Synthesis and Its Conjugation. First, the $(\text{Ag}_{29}\text{LA}_{12})^{[3-]}$ cluster (hereafter Ag_{29}) was prepared and characterized as described previously.¹⁴ The raw cluster solution was purified by sequential washing with acetone followed by extraction with methanol. Mass analysis was performed in a Bruker micrOTOF time-of-flight mass spectrometer operating in negative mode, loop injection, 50:50 methanol/water solvent flowing at 10 $\mu\text{L}/\text{min}$ (for other details, see the [Supporting Information](#)).

The cluster was conjugated to 6-APA in two steps as depicted in [Scheme S1](#) (Supporting Information) using free-base EDAC [1-ethyl-3-(3-dimethylaminopropyl)carbodiimide] as a coupling agent and sulfo-NHS [*N*-hydroxysulfosuccinimide] as a catalyst. The sulfo-ester intermediate may be precipitated and washed free of unconjugated reactants by controlling the pH. Once cleaned, the sulfo-ester cluster is redispersed in solvent by increasing its pH and subsequently reacted with the penicillanic derivative. The use of the free-base form of the activating agent was essential in conjugating the cluster. Numerous trials of the same reaction using the salt form or the HCL form of EDC were unsuccessful despite the in situ addition of two molar equivalents of the base. However, no such difficulties were encountered when conjugating the bare ligand (unattached to the cluster). Also, the 500 mM MES concentration was important to ensure the solubility of excess coupling agent and to control the pH at optimal conditions.

Bioassay and Microscopy. To measure inhibition on a preformed biofilm, we performed a phenotypic assay with some modifications.⁵² Briefly, strain of *S. aureus* UAMS-1 was cultured at 37 °C for 24 h on selective plates (ChromAgar BD Biosciences), subcultured in tryptic soy broth (TSB) liquid media on an orbital shaker at 37 °C for 18–24 h. Cells were resuspended in brain heart infusion (BHI) medium enriched with 10% human serum (HS) at 37 °C. Following incubation, the cultures were sedimented by centrifugation (3600g) for 15 min, washed twice with PBS, and resuspended in BHI and adjusted the density of the cell suspension to 1×10^7 CFU/mL. Sterile 96-well polystyrene tissue culture plates (Falcon, Franklin lakes, NJ) were inoculated with 100 μL of the bacterial suspension. Plates were incubated at 37 °C for 3 h to allow biofilm formation and attachment, the culture supernatant from each well was decanted, and planktonic cells were removed by washing with PBS. After the washing steps, 2-fold serial dilutions were prepared in the 96-well polystyrene tissue culture plate containing BHI at a final volume of 100 μL per well. The final concentration of the Ag_{29} cluster (12–0.19 mM), 6-APA (48–0.10 mM), and the conjugate (6-APA 48–

0.10 + Ag_{29} cluster 0.600–0.0011 mM) with medium without the agents as the nontreated control and the medium alone as the blank control. The viability of the biofilm on each individual well quantified by a luciferase viability assay (Presto blue) according to the manufacturer's instructions.

Visualization of *S. aureus* Biofilm by Scanning Electron Microscopy (SEM). Ultrastructural visualization of the inhibition of *S. aureus* biofilm was performed by SEM as in ref 14, in 6-well plates (Corning Incorporated, Corning, NY) with the mature biofilm treated with 6-APA, the conjugate, or $\text{Ag}_{29}\text{RALA}_{12}$ for 24 h at 37 °C. After treatment, the biofilms were washed with PBS and fixed with 4% formaldehyde and 1% glutaraldehyde in PBS at room temperature. 6-APA, the conjugate, and $\text{Ag}_{29}\text{RALA}_{12}$ were used at a concentration previously calculated to be the IC_{50} . The samples were washed twice in PBS and post-fixed at room temperature in 1% osmium tetroxide (OsO_4). For the drying of the samples, we used a graded ethanol series (25, 50, 75, and 95% ETOH). The dried specimens were then placed on copper grids to be observed with SEM in a Hitachi S-5500.

■ ASSOCIATED CONTENT

📄 Supporting Information

The Supporting Information is available free of charge at <https://pubs.acs.org/doi/10.1021/acsomega.9b02908>.

Detailed methodology is provided for cluster purification, cluster conjugation, and mass spectrometry analysis ([PDF](#))

■ AUTHOR INFORMATION

Corresponding Authors

*E-mail: Humberto.laravillegas@utsa.edu (H.H.L.).

*E-mail: alvaremm@lacitycollege.edu (M.M.A.).

*E-mail: robert.whetten@nau.edu (R.L.W.).

ORCID

Humberto H. Lara: 0000-0003-4854-9839

David M. Black: 0000-0003-2757-447X

Marcos M. Alvarez: 0000-0001-6551-8861

Robert L. Whetten: 0000-0002-9838-6823

Author Contributions

¹H.H.L. and D.M.B. contributed equally. The manuscript was written through contributions of all authors. All authors have given approval to the final version of the manuscript.

Funding

This work has been supported by The Welch Foundation Grant AX-1857 (Professor R.L.W.). Additional support was provided by the Margaret Batts Tobin Foundation, San Antonio, TX (Professor J.L.-R.).

Notes

The authors declare no competing financial interest.

■ ACKNOWLEDGMENTS

LACC Authors acknowledge valuable contributions from Miguel Brenes, Dongwan Kim, and Anthony Jeong.

■ ABBREVIATIONS

Ag_{29} , cluster $\text{Na}_3(\text{Ag}_{29}\text{LA}_{12})$; CI, combination index; ESI-MS, electrospray ionization mass spectrometry; EDC, 1-ethyl-3-(3-dimethylaminopropyl)carbodiimide; Fa, fraction affected; IC_{50} , half-maximal inhibitory concentration; LA, lipoic acid; MES, 2-(*N*-morpholino)ethanesulfonic acid; RALA, *R*(α)lipoic

acid; SEM, scanning electron microscopy; sNHS, N-hydroxysulfosuccinimide; 6-APA, 6-aminopenicillanic acid; TEA, triethylamine; TEAA, triethylammonium acetate

REFERENCES

- (1) Tong, S. Y.; Davis, J. S.; Eichenberger, E.; Holland, T. L.; Fowler, V. G. *Staphylococcus aureus* Infections: Epidemiology, Pathophysiology, Clinical Manifestations, and Management. *Clin. Microbiol. Rev.* **2015**, *28*, 603–661.
- (2) Foster, T. J. Antibiotic Resistance in *Staphylococcus aureus*. Current Status and Future Prospects. *FEMS Microbiol. Rev.* **2017**, *41*, 430–449.
- (3) Kong, K. F.; Schnepfer, L.; Mathee, K. Beta-lactam Antibiotics: from Antibiosis to Resistance and Bacteriology. *APMIS* **2010**, *118*, 1–36.
- (4) Romaniuk, J. A.; Cegelski, L. Bacterial Cell Wall Composition and the Influence of Antibiotics by Cell-Wall and Whole-cell NMR. *Philos. Trans. R. Soc., B* **2015**, *370*, No. 20150024.
- (5) Morones, J. R.; Elechiguerra, J. L.; Camacho, A.; Holt, K.; Kouri, J. B.; Ramirez, J. T.; Yacamán, M. J. The Bactericidal Effect of Silver Nanoparticles. *Nanotechnology* **2005**, *16*, 2346–2353.
- (6) Lara, H. H.; Garza-Treviño, E. N.; Ixtepan-Turrent, L.; Singh, D. K. Silver Nanoparticles are Broad-spectrum Bactericidal and Virucidal Compounds. *J. Nanobiotechnol.* **2011**, *9*, 30.
- (7) Yun'an Qing, L. C.; Li, R.; Liu, G.; Zhang, Y.; Tang, X.; Wang, J.; Liu, H.; Qin, Y. Potential Antibacterial Mechanism of Silver Nanoparticles and the Optimization of Orthopedic Implants by Advanced Modification Technologies. *Int. J. Nanomed.* **2018**, *13*, 3311.
- (8) Slavin, Y. N.; Asnis, J.; Häfeli, U. O.; Bach, H. Metal Nanoparticles: Understanding the Mechanisms Behind Antibacterial Activity. *J. Nanobiotechnol.* **2017**, *15*, 65.
- (9) Romero-Urbina, D. G.; Lara, H. H.; Velázquez-Salazar, J. J.; Arellano-Jiménez, M. J.; Larios, E.; Srinivasan, A.; Lopez-Ribot, J. L.; Yacamán, M. J. Ultrastructural Changes in Methicillin-Resistant *Staphylococcus aureus* Induced by Positively Charged Silver Nanoparticles. *Beilstein J. Nanotechnol.* **2015**, *6*, 2396–2405.
- (10) Lok, C. N.; Ho, C. M.; Chen, R.; He, Q. Y.; Yu, W. Y.; Sun, H.; Tam, P. K.; Chiu, J. F.; Che, C. M. Proteomic Analysis of the Mode of Antibacterial Action of Silver Nanoparticles. *J. Proteome Res.* **2006**, *5*, 916–924.
- (11) Durán, N.; Durán, M.; Bispo de Jesus, M.; Seabra, A. B.; Fávoro, W. J.; Nakazato, G. Silver Nanoparticles: A New View on Mechanistic Aspects on Antimicrobial Activity. *Nanomedicine* **2016**, *12*, 789–799.
- (12) Zheng, K.; Setyawati, M. I.; David, T. L.; Xie, J. Antimicrobial Silver Nanomaterials. *Coord. Chem. Rev.* **2018**, *357*, 1–17.
- (13) Wu, Y.; Yang, Y.; Zhang, Z.; Wang, Z.; Zhao, Y.; Sun, L. A Facile Method to Prepare Size-tunable Silver Nanoparticles and its Antibacterial Mechanism. *Adv. Powder Technol.* **2018**, *29*, 407–415.
- (14) Lopez, P.; Lara, H. H.; Mullins, S. M.; Black, D. M.; Ramsower, H.; Alvarez, M. M.; Williams, T. L.; Lopez-Lozano, X.; Weissker, H. C.; García, A. P.; Garzón, I. L.; et al. Tetrahedral (T) Closed-Shell Cluster of 29 Silver Atoms & 12 Lipolate Ligands, [Ag₂₉ (R- α -LA)₁₂](3-): Antibacterial and Antifungal Activity. *ACS Appl. Nano Mater.* **2018**, 1595–1602.
- (15) Azócar, M. I.; Gómez, G.; Levín, P.; Paez, M.; Muñoz, H.; Dinamarca, N. Antibacterial Behavior of Carboxylate Silver (I) Complexes. *J. Coord. Chem.* **2014**, *67*, 3840–3853.
- (16) Lara, H. H.; Romero-Urbina, D. G.; Pierce, C.; Lopez-Ribot, J. L.; Arellano-Jimenez, M. J.; Jose-Yacamán, M. Effect of Silver Nanoparticles on *Candida albicans* Biofilms: an Ultrastructural study. *J. Nanobiotechnol.* **2015**, *13*, 91.
- (17) Naik, K.; Kowshik, M. The silver lining: Towards the Responsible and Limited Usage of Silver. *J. Appl. Microbiol.* **2017**, *123*, 1068–1087.
- (18) Choi, H. S.; Liu, W.; Misra, P.; Tanaka, E.; Zimmer, J. P.; Ipe, B. I.; Bawendi, M. G.; Frangioni, J. V. Renal Clearance of Nanoparticles. *Nat. Biotechnol.* **2007**, *25*, 1165–1170.
- (19) Longmire, M.; Peter, L. C.; Hisataka, K. Clearance Properties of Nano-sized Particles and Molecules as Imaging Agents: Considerations and Caveats. *Nanomedicine* **2008**, *3*, 703–717.
- (20) Lu, Z.; Rong, K.; Li, J.; Yang, H.; Chen, R. Size-dependent Antibacterial Activities of Silver Nanoparticles Against Oral Anaerobic Pathogenic Bacteria. *J. Mater. Sci.: Mater. Med.* **2013**, *24*, 1465–1471.
- (21) Hoshyar, N.; Gray, S.; Han, H. B.; Bao, G. The Effect of Nanoparticle Size on In Vivo Pharmacokinetics and Cellular Interaction. *Nanomedicine* **2016**, *11*, 673–692.
- (22) Rolinson, G. N.; Geddes, A. M. The 50th Anniversary of the Discovery of 6-aminopenicillanic acid (6-APA). *Int. J. Antimicrob. Agents* **2007**, *29*, 3–8.
- (23) Parmar, A.; Kumar, H.; Marwaha, S. S.; Kennedy, J. F. Advances in Enzymatic Transformation of Penicillins to 6-aminopenicillanic Acid (6-APA). *Biotechnol. Adv.* **2000**, *18*, 289–301.
- (24) *The Biology of β -Lactam Antibiotics*; Morin, R. B.; Gorman, M., Eds.; Elsevier, 2014.
- (25) Li, P.; Li, J.; Wu, Q.; Li, J. Synergistic Antibacterial Effects of β -lactam Antibiotic Combined with Silver Nanoparticles. *Nanotechnology* **2005**, *16*, 1912.
- (26) Ahmed, V.; Kumar, J.; Kumar, M.; Chauhan, M. B.; Vij, M.; Ganguli, M.; Chauhan, N. S. Synthesis, Characterization of Penicillin G Capped Silver Nanoconjugates to Combat β -lactamase Resistance in Infectious Microorganism. *J. Biotechnol.* **2013**, *163*, 419–424.
- (27) Hassan, M. H. A.; Ismail, M. A.; Moharram, A. M.; Shoreit, A. Synergistic Effect of Biogenic Silver-nanoparticles with β lactam Cefotaxime against Resistant *Staphylococcus arlettae* AUMC b-163 Isolated from T3A Pharmaceutical Cleanroom, Assiut, Egypt. *Am. J. Microbiol. Res.* **2016**, *4*, 132–137.
- (28) Surwade, P.; Ghildyal, C.; Weikel, C.; Luxton, T.; Peloquin, D.; Fan, X.; Shah, V. Augmented Antibacterial Activity of Ampicillin with Silver Nanoparticles against Methicillin-resistant *Staphylococcus aureus* (MRSA). *J. Antibiot.* **2019**, *72*, 50–53.
- (29) Zheng, Y.; Liu, W.; Chen, Y.; Li, C.; Jiang, H.; Wang, X. Conjugating Gold Nanoclusters and Antimicrobial Peptides: From Aggregation-induced Emission to Antibacterial Synergy. *J. Colloid Interface Sci.* **2019**, *546*, 1–10.
- (30) Gies, A. P.; Hercules, D. M.; Gerdon, A. E.; Cliffler, D. E. Electrospray Mass Spectrometry Study of Tiopronin Monolayer-protected Gold Nanoclusters. *J. Am. Chem. Soc.* **2007**, *129*, 1095–1104.
- (31) Zuber, G.; Weiss, E.; Chipper, M. Biocompatible Gold Nanoclusters: Synthetic Strategies and Biomedical Prospects. *Nanotechnology* **2019**, *30*, No. 352001.
- (32) Safer, D.; Hainfeld, J.; Wall, J. S.; Reardon, J. E. Biospecific Labeling with Undecagold: Visualization of the Biotin-binding Site on Avidin. *Science* **1982**, *218*, 290–291.
- (33) Walter, M.; Akola, J.; Lopez-Acevedo, O.; Jadzinsky, P. D.; Calero, G.; Ackerson, C. J.; Whetten, R. L.; Grönbeck, H.; Häkkinen, H. A Unified View of Ligand-protected Gold Clusters as Superatom Complexes. *Proc. Natl. Acad. Sci. U.S.A.* **2008**, *105*, 9157–9162.
- (34) van der Linden, M.; Barendregt, A.; van Bunningen, A. J.; Chin, P. T.; Thies-Weesie, D.; de Groot, F. M.; Meijerink, A. Characterisation, Degradation and Regeneration of Luminescent Ag₂₉ Clusters in Solution. *Nanoscale* **2016**, *8*, 19901–19909.
- (35) Russier-Antoine, I.; Bertorelle, F.; Hamouda, R.; Rayane, D.; Dugourd, P.; Sanader, Z.; Bonacić-Koutecký, V.; Brevet, P. F.; Antoine, R. Tuning Ag₂₉ Nanocluster Light Emission from Red to Blue with One and Two-photon Excitation. *Nanoscale* **2016**, *8*, 2892–2898.
- (36) Kumar, J.; Kawai, T.; Nakashima, T. Circularly Polarized Luminescence in Chiral Silver Nanoclusters. *Chem. Commun.* **2017**, *53*, 1269–1272.
- (37) Hermanson, G. T. *Bioconjugate Techniques*; Academic Press, 2013.

- (38) Madison, S. A.; Carnali, J. O. PH Optimization of Amidation via Carbodiimides. *Ind. Eng. Chem. Res.* **2013**, *52*, 13547–13555.
- (39) Gruzman, A.; Hidmi, A.; Katzhendler, J.; Haj-Yehie, A.; Sasson, S. Synthesis and Characterization of New and Potent α -Lipoic Acid Derivatives. *Bioorg. Med. Chem.* **2004**, *12*, 1183–1190.
- (40) *Lipoic Acid Energy Production, Antioxidant Activity and Health Effects*; Patel, M. S.; Lester, P., Eds.; CRC Press: Boca Raton, 2008.
- (41) Shay, K. P.; Moreau, R. F.; Smith, E. J.; Smith, A. R.; Hagen, T. M. Alpha-lipoic Acid as a Dietary Supplement: Molecular Mechanisms and Therapeutic Potential. *Biochim. Biophys. Acta* **2009**, *1790*, 1149–1160.
- (42) Henderson, L. C.; Altimari, J. M.; Dyson, G.; Servinis, L.; Niranjana, B.; Risbridger, G. P. A Comparative Assessment of α -lipoic acid N-phenylamides as Non-steroidal Androgen Receptor Antagonists both on and off Gold Nanoparticles. *Bioorg. Chem.* **2012**, *40*, 1–5.
- (43) Kwiecień, B.; Dudek, M.; Bilaska-Wilkosz, A.; Knutelska, J.; Bednarski, M.; Kwiecień, I.; Zygmunt, M.; Iciek, M.; Sokolowska-Jeżewicz, M.; et al. In Vivo Anti-inflammatory Activity of Lipoic Acid Derivatives in Mice. *Postępy Hig. Med. Dosw.* **2013**, *67*, 331–338.
- (44) *The Chemistry of β -Lactams*; Page, M. L., Ed.; Springer Science & Business Media, 2012.
- (45) Schwartz, M. A. Mechanism of degradation of penicillin G in acidic solution. *J. Pharm. Sci.* **1965**, *54*, 472–473.
- (46) Deshpande, A. D.; Baheti, K. G.; Chatterjee, N. R. Degradation of β -lactam antibiotics. *Curr. Sci.* **2004**, 1684–1695.
- (47) AbdulHalim, L. G.; Bootharaju, M. S.; Tang, Q.; Del Gobbo, S.; AbdulHalim, R. G.; Eddaoudi, M.; Jiang, D. E.; Bakr, O. M. Ag₂₉(BDT)₁₂(TPP)₄: A Tetraivalent Nanocluster. *J. Am. Chem. Soc.* **2015**, *137*, 11970–11975.
- (48) Singh, R.; Shedbalkar, U. U.; Wadhvani, S. A.; Chopade, B. A. Bacteriogenic silver nanoparticles: synthesis, mechanism, and applications. *Appl. Microbiol. Biotechnol.* **2015**, *99*, 4579–4593.
- (49) Różycka, D.; Leśnikowski, Z. J.; Olejniczak, A. B. Synthesis of Boron Cluster Analogs of Penicillin and their Antibacterial Activity. *J. Organomet. Chem.* **2019**, *881*, 19–24.
- (50) Chou, T. C. Drug Combination Studies and their Synergy Quantification using the Chou-Talalay Method. *Cancer Res.* **2010**, *70*, 440–446.
- (51) Lara, H. H.; Guisbiers, G.; Mendoza, J.; Mimun, L. C.; Vincent, B. A.; Lopez-Ribot, J. L.; Nash, K. L. Synergistic Antifungal Effect of Chitosan-stabilized Selenium Nanoparticles Synthesized by Pulsed Laser Ablation in Liquids Against *Candida albicans* Biofilms. *Int. J. Nanomed.* **2018**, *13*, 2697.
- (52) Peeters, E.; Nelis, H. J.; Coenye, T. Comparison of Multiple Methods for Quantification of Microbial Biofilms Grown in Microtiter Plates. *J. Microbiol. Methods* **2008**, *72*, 157–165.